

行政院國家科學委員會專題研究計畫 成果報告

楔形含水層在不同地形邊界條件下之地下水流解析解

計畫類別：個別型計畫

計畫編號：NSC94-2211-E-009-015-

執行期間：94年08月01日至95年07月31日

執行單位：國立交通大學環境工程研究所

計畫主持人：葉弘德

計畫參與人員：張雅琪

報告類型：精簡報告

處理方式：本計畫可公開查詢

中 華 民 國 95 年 8 月 21 日

中文摘要

楔形含水層的水位分佈，與楔形含水層的角度、地形、水文地質、及抽水狀況有密切關係，其分布或許可以用假想井法(image well theory)來分析，然而假想井法限制 π 必須為楔形角度的整數倍。用數學模式模擬地下水問題時，邊界條件的設定，通常用定水頭或定流量條件來表示現地的水文地質狀況。例如一條底部與含水層相連的河流，在數學模式中，其水位分佈可用定水頭邊界條件代表。因此，一個與徑向距離有函數關係的方程式，可用來描述定水頭邊界的水位分佈。本計畫利用積分轉換(Integral transforms)方法，推導代表楔形含水層水位分佈的一個完整的解析解，此解析解可考慮有抽水狀況、邊界條件為定水頭或零流量條件的情形，且定水頭邊界也將地表坡度和起伏變化的狀況納入考慮。本研究建立的數學模式，接近現實物理世界的情形，實用性相當廣泛。

關鍵詞：楔形含水層、定水頭邊界、地下水、積分轉換。

英文摘要

The hydraulic head distribution in a wedge-shaped aquifer depends on the wedge angle, pumping rate, and the topographic and hydrogeological conditions. The solution for the hydraulic head distribution in a wedge-shaped aquifer may be obtained using the image well theory. However, the image theory is applicable only when the angle between the bounding radii expressed as π/n is restricted to that n is an integer. An equation in terms of the radial distance with trigonometric functions along the boundary may be suitable to describe the water level configuration for a valley flank with a gentle sloping and rolling topography. The project developed a general mathematical model including the governing equation and a variety of boundary conditions for the groundwater flow system within a wedge-shaped aquifer. Based on the model, a new closed-form solution for transient flow in the wedge-shaped aquifer was derived. This solution may be used to describe the head distribution for wedges that the method of images is inapplicable, and to explore the effects of the pumping or the recharge from various topographic boundaries on the flow system within a wedge-shaped aquifer.

Keywords: Wedge-shaped aquifer, constant-head boundary, groundwater, integral transform.

Introduction

Theis [5] developed a solution for evaluating drawdown during pumping test analysis in a homogeneous, isotropic and non-leaky aquifer of infinite extent. However, the well-hydraulic theory can not cope with the aquifers with impervious faults as no-flow boundaries or rivers as constant-head boundaries. In general, the solution for the hydraulic head distribution in a wedge-shaped aquifer with various boundaries may be obtained by adding imaginary wells known as the image wells. However, the image theory is applicable only when the angle between the bounding radii expressed as π/n where n is an integer [4]. Chan et al. [1] developed an analytic solution for drawdowns in rectangular aquifers. For the wedge-shaped aquifer, Chan et al. [2] applied the finite sine transform and Hankel transform to obtain the transient-state and steady-state drawdown solutions with an infinite wedge, and applied the finite sine transform and Mellin transform to obtain a steady-state drawdown solution which does not

contain an infinite series term and is much easier to compute. Chan et al. [2] only considered the case of a zero-drawdown boundary, i.e., assuming the surface topography along the boundary is flat. Kuo et al. [3] utilized the image-well method to predict the drawdown distribution in aquifers with irregularly shaped boundaries; however, their solutions may diverge if insufficient number and improper locations of the image wells are employed.

Consider a non-leaky aquifer whose plan view is a sector of a circle. The groundwater flow in a wedge-shaped aquifer is analyzed in the polar coordinate system. Physically, a groundwater flow system with a wedge-shaped aquifer is commonly formed by ancient alluvial fan. The hydraulic head distribution within the sector naturally depends on the wedge angle and boundary conditions. The constant-head and no-flow boundary conditions are often used to represent the real-world hydrogeological boundary conditions. An annual average water level for a stream may be used as the boundary of time-independent head for a regional groundwater flow system if the bottom of the stream is connected with the aquifer. For a valley flank with a gentle sloping and rolling topography, an equation in terms of the trigonometric functions of radial distance along the boundary may be suitable to describe the water level configuration [6]. The purpose of this paper is to develop a general mathematical model with a variety of topographic and hydrogeological boundary conditions to describe the groundwater flow system in a wedge-shaped aquifer. In addition, the transient-state and steady-state solutions are derived based on the mathematical model and simplified to concise forms for easy computing. Several case studies are demonstrated in this paper and those cases may be considered as the applications of the solutions.

These new solutions are useful and valuable to analyze the groundwater flow in the wedge-shaped aquifer. These solutions can be used: (1) to describe the groundwater flow in a wedge-shaped aquifer under a variety of topographic and hydrogeological boundary conditions, (2) to predict drawdown for any wedge angle of the aquifer that the traditional method of image is not applicable, (3) to evaluate the sensitivity of the parameters in the mathematical model, and (4) to identify the hydraulic parameters when coupling with an optimization approach in aquifer data analysis.

Mathematical Model

Governing Equation and Related Boundary and Initial Conditions

Figure 1 shows a wedge-shaped aquifer with an angle of ϕ and the boundaries of time-independent heads $p(r)$ and $q(r)$. These equations $p(r)$ and $q(r)$ represent the upper and lower boundaries with various topographic conditions, respectively. For a pumping well located at the point (r_0, θ_0) with a pumping rate Q , the differential equation governing the hydraulic head h at any point (r, θ) may be expressed as [2]

$$T\left(\frac{\partial^2 h}{\partial r^2} + \frac{1}{r} \frac{\partial h}{\partial r} + \frac{1}{r^2} \frac{\partial^2 h}{\partial \theta^2}\right) - S \frac{\partial h}{\partial t} = -\frac{Q}{r} \delta(r - r_0) \delta(\theta - \theta_0) \quad (1)$$

where T is the transmissivity (L^2/T); S is the storage coefficient; h is the hydraulic head (L); t is time from the start of the pumping test (T); r is the radial distance from the origin (L); and θ is the angle (radians) from the lower boundary. Figure 2 shows the hydraulic head $h(r, \theta)$

along the boundary of time-independent head (e.g. a stream or a river) consisting of three components: h_0 , h_1 and h_2 for representing a gentle sloping and rolling configuration where h_0 is a constant denoting the depth from the bottom of the aquifer. In addition, $h_1 = r \tan \alpha$ where α is the average slope of the boundary and h_2 may be approximated by [6]

$$h_2 = a \frac{\sin(br / \cos \alpha)}{\cos \alpha} \quad (2)$$

where a is the amplitude of the sine curve, $b = 2\pi / \lambda$ is the frequency, and λ is the period of the sine wave. Upon introducing the abbreviations $\tan \alpha = c'$, $a / \cos \alpha = a'$ and $b / \cos \alpha = b'$, the equations representing the hydraulic head of the lower and upper boundaries illustrated in Fig. 1 may be respectively written as:

$$h(r, \theta) = p(r) = h_p + c'_1 r + a'_1 \sin(b'_1 r), \quad \theta = 0, \quad 0 \leq r \leq \infty \quad (3)$$

and

$$h(r, \theta) = q(r) = h_q + c'_2 r + a'_2 \sin(b'_2 r), \quad \theta = \phi, \quad 0 \leq r \leq \infty \quad (4)$$

where h_p and h_q are the depth to the impervious strata for the lower and upper boundaries at the origin of the wedge-shaped aquifer, respectively. Also, the subscripts 1 and 2 denote the lower and upper boundaries respectively. In reality, h_p is equal to h_q for general cases; however, h_p and h_q may not be the same if there exists a fault at the origin of the wedge-shaped aquifer. The initial condition, shown in Appendix A, is assumed as the solution of solving (1) when omitting $\partial h / \partial t$ and setting the pumping rate Q to be zero and with the boundary conditions of (3) and (4).

Analytical Solutions for Transient-state and Steady-state Problems

Since the governing equation, the initial condition and boundary conditions are specified, the solution of hydraulic head in a wedge-shaped aquifer with an infinite radius can be obtained via the finite sine transform and Hankel transform for (1) - (4). Detailed derivations for transient-state and steady-state solutions are given in Appendix A and the results are

$$h(r, \theta, t) = \frac{2}{\phi} \sum_{n=1}^{\infty} \sin(\mu_n \theta) \left[\frac{Q}{T} \sin(\mu_n \theta_0) (\Omega_1 + \Omega_2) + \mu_n (c'_1 - (-1)^n c'_2) \Omega_3 \right. \\ \left. + \mu_n (a'_1 \Omega_4 - (-1)^n a'_2 \Omega_5) + \mu_n (h_p - (-1)^n h_q) \Omega_6 \right] \quad (5)$$

and

$$h(r, \theta) = \frac{2}{\phi} \sum_{n=1}^{\infty} \sin(\mu_n \theta) \left[\frac{Q}{T} \sin(\mu_n \theta_0) \Omega_2 + \mu_n (c'_1 - (-1)^n c'_2) \Omega_3 \right. \\ \left. + \mu_n (a'_1 \Omega_4 - (-1)^n a'_2 \Omega_5) + \mu_n (h_p - (-1)^n h_q) \Omega_6 \right] \quad (6)$$

respectively, with

$$\Omega_1 = \int_0^{\infty} \left[-\exp\left(\frac{-u^2 T}{S} t\right) \right] J_{\mu_n}(ur_0) J_{\mu_n}(ur) \frac{du}{u} \quad (7)$$

$$\Omega_2 = \int_0^{\infty} J_{\mu_n}(ur_0) J_{\mu_n}(ur) \frac{du}{u} \quad (8)$$

$$\Omega_3 = \int_0^{\infty} \frac{J_{\mu_n}(ur)}{u} \int_0^{\infty} J_{\mu_n}(u\kappa) d\kappa du \quad (9)$$

$$\Omega_4 = \int_0^{\infty} \frac{J_{\mu_n}(ur)}{u} \int_0^{\infty} \sin(b'_1 \kappa) \frac{J_{\mu_n}(u\kappa)}{\kappa} d\kappa du \quad (10)$$

$$\Omega_5 = \int_0^{\infty} \frac{J_{\mu_n}(ur)}{u} \int_0^{\infty} \sin(b'_2 \kappa) \frac{J_{\mu_n}(u\kappa)}{\kappa} d\kappa du \quad (11)$$

$$\Omega_6 = \int_0^{\infty} \frac{J_{\mu_n}(ur)}{u} \int_0^{\infty} \frac{J_{\mu_n}(u\kappa)}{\kappa} d\kappa du \quad (12)$$

and

$$\mu_n = \frac{n\pi}{\phi} \quad (13)$$

where u and κ are the dummy variables, and $J_{\mu_n}(\cdot)$ is the Bessel function of the first kind with order μ_n . The first and second terms (contain Ω_1 and Ω_2 respectively) on the right-hand side (RHS) of (5) represent the drawdown due to pumping, and the other terms represent the hydraulic head arisen from the slopes, curves, and elevations of the boundaries of the wedge-shaped aquifer respectively.

Notice that the presence of the Bessel functions of high order and large argument in (5) and (6) may be difficult to evaluate. Thus (5) and (6) are further simplified. The results for transient-state and steady-state solutions can be written as

$$\begin{aligned}
h(r, \theta, t) = & \frac{2}{\phi} \sum_{n=1}^{\infty} \sin(\mu_n \theta) \left[\frac{Q}{T} \sin(\mu_n \theta_0) \Omega_1 \right] + \frac{Q}{4\pi T} (\log \gamma_1 - \log \gamma_2) \\
& + \frac{r}{\sin \phi} \{c'_1 \sin(\phi - \theta) + c'_2 \sin(\theta)\} + \varphi [a'_1 \Lambda_1 + a'_2 \Lambda_2] \\
& + \left[\frac{\theta}{\phi} (h_q - h_p) + h_p \right]
\end{aligned} \tag{14}$$

and

$$\begin{aligned}
h(r, \theta) = & \frac{Q}{4\pi T} (\log \gamma_1 - \log \gamma_2) \\
& + \frac{r}{\sin \phi} \{c'_1 \sin(\phi - \theta) + c'_2 \sin(\theta)\} + \varphi [a'_1 \Lambda_1 + a'_2 \Lambda_2] \\
& + \left[\frac{\theta}{\phi} (h_q - h_p) + h_p \right]
\end{aligned} \tag{15}$$

respectively, with

$$\Lambda_1 = \int_0^{\infty} \frac{u^{(\pi/\phi)-1} \sin(b'_1 u)}{\psi_1} du \tag{16}$$

$$\Lambda_2 = \int_0^{\infty} \frac{u^{(\pi/\phi)-1} \sin(b'_2 u)}{\psi_2} du \tag{17}$$

$$\psi_1 = u^{2\pi/\phi} - 2r^{\pi/\phi} u^{\pi/\phi} \cos\left(\frac{\pi}{\phi} \theta\right) + r^{2\pi/\phi} \tag{18}$$

$$\psi_2 = u^{2\pi/\phi} + 2r^{\pi/\phi} u^{\pi/\phi} \cos\left(\frac{\pi}{\phi} \theta\right) + r^{2\pi/\phi} \tag{19}$$

$$\varphi = \frac{r^{\pi/\phi} \sin\left(\frac{\pi}{\phi} \theta\right)}{\phi} \tag{20}$$

$$\gamma_1 = 1 - 2\left(\frac{r}{r_0}\right)^{\pi/\phi} \cos\frac{\pi(\theta + \theta_0)}{\phi} + \left(\frac{r}{r_0}\right)^{2\pi/\phi} \tag{21}$$

and

$$\gamma_2 = 1 - 2\left(\frac{r}{r_0}\right)^{\pi/\phi} \cos\frac{\pi(\theta - \theta_0)}{\phi} + \left(\frac{r}{r_0}\right)^{2\pi/\phi} \tag{22}$$

If $r > r_0$, the solution can be obtained by interchanging r and r_0 in both (21) and (22). Like the term in (5), the first and second terms on the right-hand side (RHS) of (14) represent the drawdown due to pumping, and the other terms represents the hydraulic head arisen from the slopes, curves and elevations of the boundaries of the wedge-shaped aquifer respectively. Equations (14) and (15) can be evaluated more easily and quickly than (5) and (6).

Problem with an impervious boundary condition

The problem with an impervious boundary at the lower wedge is shown in Fig. 3. The solution can be obtained by replacing ϕ with 2ϕ , setting the topographic parameters at the lower wedge to be zero, and inserting a second pumping well at the point $(r_0, 2\phi - \theta_0)$ in (14) and (15). For the time dependent component in (14), $\mu_{\frac{n+1}{2}} = (2n+1)\pi/2\phi$ is used to replace

$\mu_n = n\pi / \phi$. Thus, the transient-state and steady-state solutions for a wedge-shaped aquifer with an upper boundary of time-independent head and a lower impervious boundary can be expressed as

$$h(r, \theta, t) = \frac{1}{\phi} \sum_{n=1}^{\infty} \sin(\mu_{n+\frac{1}{2}} \theta) \left[\frac{Q}{T} \sin(\mu_{n+\frac{1}{2}} \theta_0) \Omega_1 \right] + \frac{Q}{4\pi T} (\log \gamma'_1 - \log \gamma'_2) + \frac{1}{\phi} \sum_{n=1}^{\infty} \sin(\mu_{n+\frac{1}{2}} \theta) \left[\frac{Q}{T} \sin(\mu_{n+\frac{1}{2}} (2\phi - \theta_0)) \Omega_1 \right] + \frac{Q}{4\pi T} (\log \gamma_3 - \log \gamma_4) + \frac{c'_1 r \cos(\phi - \theta)}{\cos \phi} + \varphi' a'_1 \Lambda'_1 + h_p \quad (23)$$

and

$$h(r, \theta) = \frac{Q}{4\pi T} (\log \gamma'_1 - \log \gamma'_2) + \frac{Q}{4\pi T} (\log \gamma_3 - \log \gamma_4) + \frac{c'_1 r \cos(\phi - \theta)}{\cos \phi} + \varphi' a'_1 \Lambda'_1 + h_p \quad (24)$$

respectively, where

$$\Lambda'_1 = \int_0^{\infty} \frac{(u^{(3\pi/\phi)-1} + r^{\pi/\phi} u^{\pi/2\phi}) \sin(b'_1 u)}{\psi_1} du \quad (25)$$

$$\varphi' = \frac{r^{\pi/2\phi} \sin(\frac{\pi}{2\phi} \theta)}{\phi} \quad (26)$$

$$\gamma'_1 = 1 - 2 \left(\frac{r}{r_0} \right)^{\pi/2\phi} \cos \frac{\pi(\theta + \theta_0)}{2\phi} + \left(\frac{r}{r_0} \right)^{\pi/\phi} \quad (27)$$

$$\gamma'_2 = 1 - 2 \left(\frac{r}{r_0} \right)^{\pi/2\phi} \cos \frac{\pi(\theta - \theta_0)}{2\phi} + \left(\frac{r}{r_0} \right)^{\pi/\phi} \quad (28)$$

$$\gamma_3 = 1 - 2 \left(\frac{r}{r_0} \right)^{\pi/2\phi} \cos \frac{\pi(\theta + 2\phi - \theta_0)}{2\phi} + \left(\frac{r}{r_0} \right)^{\pi/\phi} \quad (29)$$

and

$$\gamma_4 = 1 - 2 \left(\frac{r}{r_0} \right)^{\pi/2\phi} \cos \frac{\pi(\theta - 2\phi + \theta_0)}{2\phi} + \left(\frac{r}{r_0} \right)^{\pi/\phi} \quad (30)$$

If $r > r_0$, the solution can be obtained by interchanging r and r_0 in (27) - (30).

Results and Discussion

Several cases are considered in this paper. Table 1 lists the wedge angle and the topographical parameters for cases (a) - (c) as the ancient alluvial fans with various boundaries.

Assume that there is a single pumping well located at $r_0 = 1000$ m and $\theta_0 = 30^\circ$ in these alluvial fans with a pumping rate $30,000 \text{ m}^3/\text{day}$ for two days. These cases can be regarded as the applications of the analytical solutions. The configurations of the hydraulic head distribution for cases (a) - (c) are also shown in Figs. 4(a) – 7(c) respectively. Different angles of the wedge-shaped aquifer and topographic parameters of the rechargeable boundaries cause significantly different configurations of the hydraulic head distribution within the wedge-shaped aquifer.

Figure 5 demonstrates the transient-state drawdown of the wedge-shaped aquifer for a pumping well located at $(1000,30^\circ)$ with the pumping rate $30,000 \text{ m}^3/\text{day}$ and two observation wells located at $(900,30^\circ)$ and $(1200,45^\circ)$ respectively with the boundary of time-independent head. These curves indicate that the drawdown increases with time, and the system tends to reach steady-state after 100 hours at $(900,30^\circ)$ and after 150 hours at $(1200,45^\circ)$.

Conclusions

A mathematical model for a wedge-shaped aquifer with various topographic and hydrogeological boundary conditions is presented. These solutions are derived via the Fourier finite sine transform and the Hankel transform. These solutions are further simplified to concise forms for easy computing. This paper extends the boundary conditions of the problem investigated by Chan et al. [2] to a more general case. In addition, this paper also improves the results of Chan et al. and simplifies some of their expressions to allow for easier numerical evaluation. New formulas (37)-(39) relate the steady-state solution derived via the Hankel transform to the solution derived via the Mellin transform in Chan et al. [2]. The transient-state solution consists of an infinite series containing an infinite integral of Bessel functions and the steady-state solution also consists of an infinite integral of trigonometric functions.

These newly derived solutions may have advantages of serving the following purposes: (1) to describe the groundwater flow in a wedge-shaped aquifer under various topographic and hydrogeological boundary conditions, (2) to predict drawdown for any wedge angle of the aquifer that the traditional method of image is not applicable, (3) to evaluate the sensitivity of the parameters in the mathematical model, and (4) to identify the hydraulic parameters when coupling with an optimization approach in aquifer data analysis.

References

- [1] Chan YK, Mullineux N, Reed JR. Analytical solutions for drawdowns in rectangular artesian aquifers. *J Hydrol* 1976; 31:151-160.
- [2] Chan YK, Mullineux N, Reed JR, Wells GG. Analytic solutions for drawdowns in wedge-shaped artesian aquifers. *J Hydrol* 1978; 36:233-246.
- [3] Kuo MCT, Wang WL, Lin DS, Chiang CJ. An image-well method for predicting drawdown distribution in aquifers with irregularly shaped boundaries. *Ground Water* 1994; 32(5): 794-804.
- [4] Schwartz FW, Zhang H. Fundamentals of ground water. New York: John Wiley & Sons Inc.;2003.
- [5] Theis CV. The relation between the lowering of the piezometric surface and the rate and duration of discharge of a well using ground-water storage. *Eos Trans AGU* 1935; 16: 519-524.
- [6] Toth J. A theoretical analysis of groundwater flow in small drainage basins. *J Geophysical research* 1963; 68(16): 4795-4813.

Table 1. The wedge angle and the topographical parameters of the boundary of time-independent head for various cases

Case	Wedge angle	Topographical parameters for lower and upper boundaries			
	ϕ	^a a_1/a_2	^b b_1/b_2	^c α_1/α_2	^d h_1/h_2
a	60°	10 / 10	0.004 / 0.004	1.14° / 1.14°	100 / 100
b	120°	10 / 15	0.004 / 0.008	1.14° / 0.57°	100 / 85
c	47°	10 / 15	0.004 / 0.008	1.14° / 0.57°	100 / 85

^a a represents the amplitude of the sine curve for the boundary.

^b b represents the frequency for the boundary.

^c α represents the average slope for the boundary.

^d h represents the depth for the boundary at the origin of the wedge-shaped aquifer.

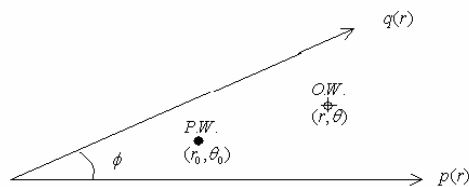


Fig. 1. The infinite wedge with boundary of time-independent head

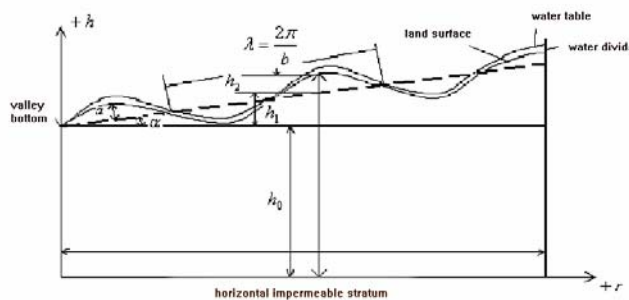


Fig. 2. Idealized cross section of a valley flank in a small drainage basin

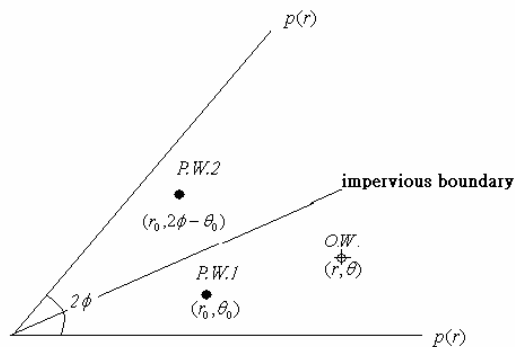
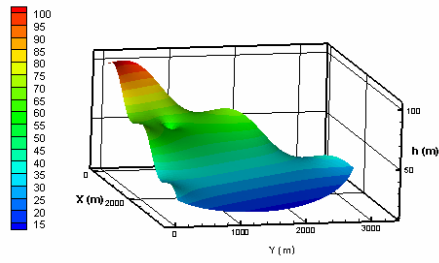
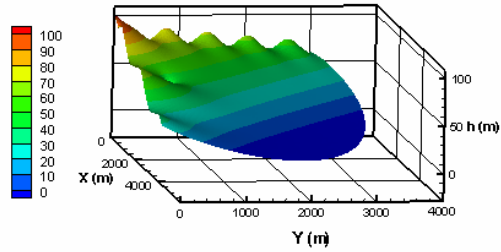


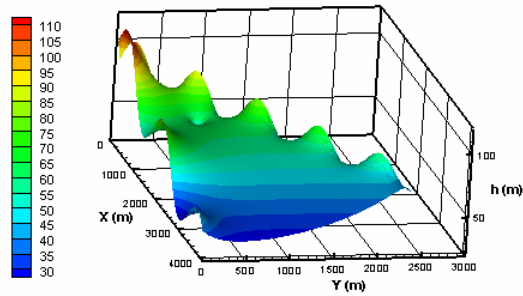
Fig. 3. The infinite wedge with impervious boundary at $\theta = \phi$



(a)



(b)



(c)

Fig. 4. Hydraulic head distributions for cases (a) - (c)

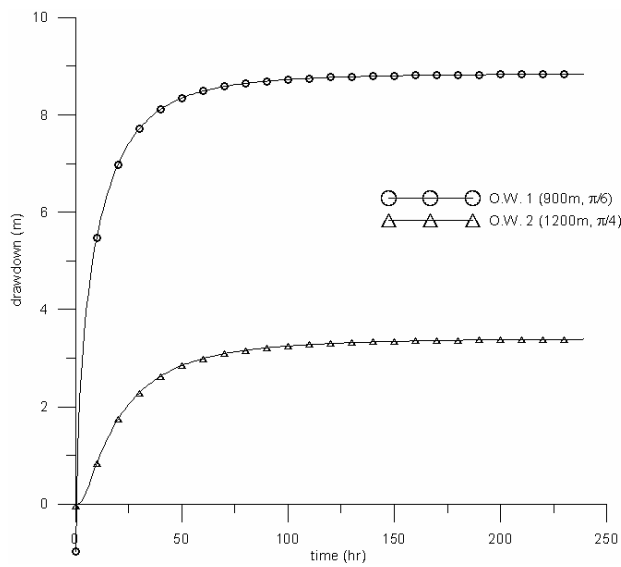


Fig. 5 The transient state drawdown for the wedge-shaped aquifer with rechargeable boundaries